Inorg. Chem. **1983**, *22*, 2825–2832

Contribution from the Department of Inorganic Chemistry,
Indian Association for the Cultivation of Science, Calcutta 700032, India

Chemistry of Ruthenium. 12.[1] Reactions of Bidentate Ligands with Diaquobis[2-(arylazo)pyridine]ruthenium(II) Cation. Stereoretentive Synthesis of Tris Chelates and Their Characterization: Metal Oxidation, Ligand Reduction, and Spectroelectrochemical Correlation

SREEBRATA GOSWAMI, RABINDRANATH MUKHERJEE, and ANIMESH CHAKRAVORTY*

Received January 11, 1983

Two isomers of the diaquo complex $Ru(OH_2)_2L_2^{2+}$, viz., trans-cis (tc) and cis-cis (cc) in the pairs N(pyridine), N(pyridine) and N(azo), N(azo), have been used to carry out the title reaction in the cases of both symmetrical and unsymmetrical bidentate ligands (B): major emphasis is given on the tc isomer [L = 2-(phenylazo)pyridine (pap) or 2-(*m*-tolylazo)pyridine (tap)]. The tris chelates thus formed are of type $RuBL_2^{x+}$ (x = 1 or 2). Using ^1H NMR data (δ_{Me} of tap complexes), one can demonstrate that the stereochemistry of the RuL_2 fragment in the tris chelates is the same as that in the parent diaquo complex. In the particular case of RuL_3^{2+}, the tc parent gives only the meridional isomer, but the cc isomer produces both meridional and facial isomers, the latter being formed in less than statistical quantities due to steric inhibition. The metal oxidation and ligand reduction behavior of the complexes are studied electrochemically in acetonitrile. High (0.7–2.3 V) formal potentials for the ruthenium(III)–ruthenium(II) couple are generally observed. In the case of $Ru(acac)(tap)_2^+$, the ruthenium(IV)–ruthenium(III) couple occurs near 2 V. In $Ru(en)(tap)_2^{2+}$, secondary oxidation of en follows electrochemical metal oxidation. Short Ru–N distances are correlated with high ruthenium(III)–ruthenium(II) formal potentials. The Ru–N(azo) bond is shorter than the Ru–N(pyridine) bond due to greater π-back-bonding in the former case. The high potentials of the present complexes are thus related to the strong Ru–N(azo) π-bonding. For the triazene 1-oxide complexes $Ru(EtN(O)NNC_6H_4R\text{-}p)(pap)_2^+$, R has been systematically varied from strongly electron donating (OMe) to strongly electron withdrawing (NO_2). The formal potentials obey the Hammett relationship very well. Ligand-based reductions are investigated at hanging mercury drop electrode in the range 0 to −2.7 V. In RuL_3^{2+}, six such reductions constitute the complete electron-transfer series. The electrons are believed to be added successively to the three azo functions. In the mixed chelates $Ru(bpy)L_2^{2+}$ and $Ru(bpy)_2L^{2+}$, both bpy and L reductions are observed. A correlation of MLCT transition energy with the difference between the formal potentials of the ruthenium(III)–ruthenium(II) couple and the first ligand reduction couple is noted. The energy of the MLCT band is predictable to within ±1000 cm^{-1} of the experimental value.

Introduction

Interesting patterns of structure and reactivity in ruthenium chemistry are emerging from recent studies[2–6] of the complexes of 2-(arylazo)pyridines (L), **1**. Two such ligands have been used so far: 2-(phenylazo)pyridine (pap) and 2-(*m*-tolylazo)pyridine (tap). The tap complexes are particularly useful[3] where proton NMR (δ_{Me}) is utilized as a structural probe. The ligand L is a potent π-acceptor[3,6]—more potent than 2,2′-bipyridine (bpy). Strong M–L back-bonding therefore characterizes complexes of L with "electron-rich" metal ions such as iron(II),[7] ruthenium(II),[3,6] osmium(II),[8] palladium(II),[8] and copper(I).[9] The effect is seen in vibration frequencies[3,6–9] ($\nu_{N=N}$), charge-transfer spectra,[3,6–9] and proton dissociation constants[3,4] and more directly in bond distance data.[3,10]

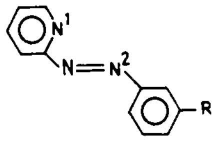

R = H ; L = pap
R = Me ; L = tap

1

In general, the dihalo chelate[2a,5] RuX_2L_2 (X = Cl, Br, I) is formed by the reaction of L with RuX_3. It is the source material for generating new Ru–L complexes. Five isomers are possible for RuX_2L_2. Of these, three—one green and the other two blue—have been realized in the cases of $RuCl_2L_2$ and $RuBr_2L_2$. The RuI_2L_2 complex appears to exist in the green form only. The stereochemistry of the isomers can be defined[3] by setting the relative positions (cis (*c*) or trans (*t*)) in the pair N^1, N^1 and in the pair N^2, N^2. It is now established[2–6,10] that the stereochemistries of the three isomers of RuX_2L_2 are *tt* (green), *tc* (blue), and *cc* (blue).

Tertiary phosphines displace halides from RuX_2L_2 stereodynamically, i.e., with change in RuL_2 stereochemistry via S_N2 edge-displacement pathways.[2b,11] On the other hand, halide displacement by H_2O (reaction 1) in the presence of aqueous

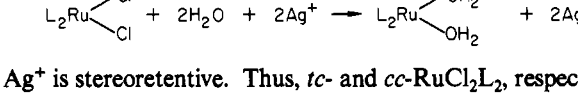

$$L_2RuCl_2 + 2H_2O + 2Ag^+ \rightarrow L_2Ru(OH_2)_2^{2+} + 2AgCl \quad (1)$$

Ag^+ is stereoretentive. Thus, *tc*- and *cc*-$RuCl_2L_2$, respectively, give rise[3] to *tc*- and *cc*-$Ru(OH_2)_2L_2^{2+}$ (**2** and **3**). The aqua molecules in **2** and **3** are labile, and this makes the latter two species potentially excellent starting materials for the synthesis of a variety of complexes of RuL_2^{2+}. Thus, **2** and **3** undergo facile solvolysis,[3] producing $RuS_2L_2^{2+}$ (S = $HC(O)NMe_2$,

---

[1] Part 11 is ref 32. Part 10: Mukherjee, R. N.; Chakravorty, A. *J. Chem. Soc., Dalton Trans.*, in press.

[2] (a) Goswami, S.; Chakravarty, A. R.; Chakravorty, A. *Inorg. Chem.* **1981**, *20*, 2246. (b) *Ibid.* **1982**, *21*, 2737.

[3] Goswami, S.; Chakravarty, A. R.; Chakravorty, A. *Inorg. Chem.* **1983**, *22*, 602.

[4] Goswami, S.; Chakravarty, A. R.; Chakravorty, A. *J. Chem. Soc., Chem. Commun.* **1982**, 1288.

[5] Krause, R. A.; Krause, K. *Inorg. Chem.* **1980**, *19*, 2600.

[6] Krause, R. A.; Krause, K. *Inorg. Chem.* **1982**, *21*, 1714.

[7] Raghavendra, B. S.; Chakravorty, A. *Indian J. Chem., Sect. A* **1976**, *14A*, 166.

[8] Ghosh, B. K.; Bandyopadhyay, D.; Goswami, S.; Bandyopadhyay, P.; Chakravorty, A., unpublished results.

[9] Datta, D.; Chakravorty, A. *Inorg. Chem.* **1983**, *22*, 1611.

[10] Seal, A.; Ray, S., private communication.

[11] In the reaction with PMe_2Ph (abbreviated as P) the *tt*-$RuCl_2L_2$ fragment is transformed[2b] to *tc*-$RuClPL_2^+$. On the other hand, *tc*-$RuCl_2L_2$ and *cc*-RuL_2Cl_2 respectively give *cc*-$RuClPL_2^+$ and *tc*-$RuClPL_2^+$. The results are all in agreement with the edge-displacement pathway (Goswami, S.; Chakravarty, A. R.; Chakravorty, A., unpublished results).

0020-1669/83/1322-2825$01.50/0

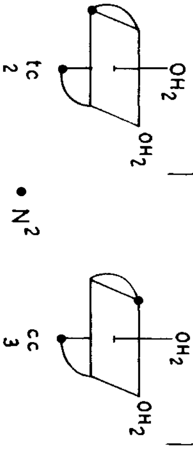

Me_2SO, RCN, pyridine (py), etc.). Particularly interesting is the half-solvolyzed complex $Ru(OH_2)(py)(pap)_2^{2+}$, which catalyzes[3,4] the oxidation of water to dioxygen by Ce^{4+} via the intermediacy of $Ru(O)(py)(pap)_2^{2+}$.

In the present work we examine reactions of $Ru(OH_2)_2L_2^{2+}$ (both **2** and **3**, mainly **2**) with a number of neutral and mononanionic bidentate ligands (B). The isomerically pure mixed tris chelates, $RuBL_2^{x+}$ (x = 1 or 2), generated in this way have been characterized as perchlorate salts. The stereochemistries have been established with the help of ^1H NMR data. Recently, isomeric mixtures of a few $Ru(B)(pap)_2^{x+}$ species have been synthesized by another group using a different route.[6] This group has considered at length the IR and charge-transfer spectra of the isomeric mixtures in terms of the π-acidities of pap and B. We therefore consider these topics only briefly.

The complexes provide a unique opportunity for probing redox reactions pertaining to both metal oxidation (reaction 2) and ligand reduction (reaction 3). The chelates are explored as carriers[12] of complete electron-transfer series. The systematics of the redox potentials of the two couples are examined with the hope of finding a correlation between spectroscopic and redox parameters.

$$Ru^{III}L + e^- \rightleftharpoons Ru^{II}L \qquad (2)$$

$$Ru^{II}L + e^- \rightleftharpoons Ru^{II}L^- \qquad (3)$$

Results and Discussion

Synthesis and Characterization. Both symmetrical and unsymmetrical bidentate ligands (B) have been used by us. The symmetrical ligands are bpy, ethylenediamine (en), and acetylacetone (Hacac). A group of triazene 1-oxides[13] ($EtN(O)NNC_6H_4R$-p^-, abbreviated as Rto), pap, and tap are used as unsymmetrical ligands. The reaction of $Ru(OH_2)_2L_2^{2+}$ with B proceeds smoothly in methanol.[14] The diaquo complex is first solvolyzed without change in stereochemistry[3] followed by displacement of methanol by B (reaction 4). The tris chelates are isolated as dark colored diamagnetic highly crystalline perchlorate monohydrate salts.

$$Ru(OH_2)_2L_2^{2+} + B \xrightarrow{MeOH} RuBL_2^{x+} + 2H_2O \qquad (4)$$

Elemental composition, solution electrical conductivity, selected infrared frequencies, and the electronic bands of the complexes are set out in Table I. Significant results are (i) the relatively low values of $\nu_{N=N}$ evidently due to[2,3,5,6] Ru → L π-donation in the ground state and (ii) one or more allowed electronic bands generally falling in the range 450–750 nm due to $t_2(Ru) \rightarrow \pi^*(L)$ charge transfer.[2,3,5,6]

Stereochemistry. The ^1H NMR signals of tap complexes were used to probe their stereochemistry. Relevant data are given in Table II and Figure 1.

(a) Case of Symmetrical and Unsymmetrical B. When B is symmetrical (bpy, en, acac⁻), a single methyl signal is always observed for the complexes obtained from tc-$Ru(OH_2)_2(tap)_2^{2+}$ (**2**). Thus, the twofold axis of **2** is retained in $Ru(B)(tap)_2^{x+}$

Table I. Molar Conductivity and Selected Infrared, Visible-Ultraviolet, and Microanalytical Data

compd	Λ_M,[a] Ω^{-1} cm² M⁻¹	IR,[b,c] ν_{max}, cm⁻¹		vis-UV,[a] λ_{max}, nm ($10^{-3}\epsilon$, M⁻¹ cm⁻¹)	anal.[e]		
		C=N	N=N		% C	% H	% N
tc-$[Ru(bpy)(pap)_2](ClO_4)_2 \cdot H_2O$	370	1595	1345	514 (9.27), 436[d] (4.20), 368 (20.60), 312[d] (20.60), 282 (30.57), 218 (29.62)	45.29 (45.70)	3.22 (3.40)	12.96 (13.32)
tc-$[Ru(bpy)(tap)_2](ClO_4)_2 \cdot H_2O$	350	1600	1340	512 (10.25), 372 (23.80), 308[d] (22.40), 280 (31.50), 216 (37.80)	47.29 (47.00)	3.77 (3.68)	13.16 (12.90)
tc-$[Ru(bpy)(tap)_2](ClO_4)_2 \cdot H_2O$	350	1600	1340	510 (10.40), 364 (24.25), 314[d] (23.90), 288 (32.25)	47.15 (47.00)	3.62 (3.68)	13.23 (12.90)
tc-$[Ru(en)(tap)_2](ClO_4)_2 \cdot H_2O$	340	1605	1325	538 (14.30), 508[d] (10.80), 360 (15.82), 308 (19.71), 290 (19.90), 218 (26.86)	40.83 (40.41)	4.21 (4.14)	14.63 (14.50)
mer-$[Ru(pap)_3](ClO_4)_2 \cdot H_2O$	380	1595	1355	492 (12.16), 464[d] (11.00), 368 (32.36), 320[d] (20.30), 278 (21.15), 218 (33.20)	45.32 (45.67)	3.39 (3.34)	14.63 (14.53)
mer-$[Ru(tap)(pap)_2](ClO_4)_2 \cdot H_2O$	400	1600	1355	492 (11.40), 464[d] (10.35), 370 (30.10), 320[d] (18.10), 276 (19.30), 218 (32.68)	46.73 (46.30)	3.50 (3.52)	14.42 (14.30)
mer-$[Ru(tap)_3](ClO_4)_2 \cdot H_2O$	390	1600	1350	494 (13.90), 464[d] (13.05), 372 (38.10), 320[d] (22.70), 278 (26.70), 216 (42.10)	47.47 (47.51)	3.72 (3.85)	13.50 (13.86)
mer-$[Ru(pap)(tap)_2](ClO_4)_2 \cdot H_2O$	390	1605	1355	492 (13.10), 464[d] (12.15), 372 (34.30), 320[d] (20.90), 278 (23.45), 218 (39.40)	46.72 (46.92)	3.42 (3.69)	14.23 (14.08)
tc-$[Ru(acac)(tap)_2]ClO_4 \cdot H_2O$	132	1600	1305	564 (12.70), 366[d] (18.30), 322 (22.64), 264[d] (16.15)	50.40 (49.90)	4.41 (4.35)	11.52 (11.81)
tc-$[Ru(OMeto)(pap)_2]ClO_4 \cdot H_2O$	128	1590	1285	710 (2.10), 552 (7.00), 348[d] (19.70), 318 (21.70), 216 (30.40)	47.91 (47.78)	3.94 (4.11)	16.57 (16.18)
tc-$[Ru(Meto)(pap)_2]ClO_4 \cdot H_2O$[f,g]	136	1590	1290	728 (1.90), 552 (7.60), 360[d] (18.70), 318 (21.70), 216 (30.40)	48.52 (48.78)	3.85 (4.20)	16.59 (16.52)
tc-$[Ru(Hto)(tap)_2]ClO_4 \cdot H_2O$	140	1580	1290	748 (2.55), 552 (9.16), 316 (23.60), 252[d] (21.50), 218 (31.80)	49.12 (49.45)	4.20 (4.38)	15.97 (16.22)
tc-$[Ru(Hto)(pap)_2]ClO_4 \cdot H_2O$	142	1590	1290	730[d] (1.50), 550 (6.70), 364[d] (16.40), 318 (21.90), 218 (28.60)	48.53 (48.09)	4.00 (4.01)	17.01 (16.83)
tc-$[Ru(Clto)(pap)_2]ClO_4 \cdot H_2O$	126	1590	1290	714 (1.90), 550 (7.40), 360[d] (18.70), 316 (22.50), 218 (29.80)	46.02 (45.97)	3.72 (3.70)	16.10 (16.09)
tc-$[Ru(CO_2Etto)(pap)_2]ClO_4 \cdot H_2O$[f,g]	118	1590	1310	716 (2.20), 548 (7.60), 362[d] (20.70), 320 (22.90), 272[d] (18.00), 216 (27.60)	48.21 (48.26)	4.07 (4.14)	15.39 (15.35)
tc-$[Ru(NO_2to)(pap)_2]ClO_4 \cdot H_2O$	132	1575	1310	710 (2.30), 540 (7.70), 452[d] (11.50), 360 (29.00), 316[d] (23.20), 216 (30.40)	45.42 (45.36)	3.48 (3.65)	18.05 (17.64)

[a] Solvent is MeCN. [b] In KBr disk (4000–400 cm⁻¹). [c] All bands are sharp and strong. [d] Shoulder. [e] Calculated values are in parentheses. [f] Electronic spectral data of coulometrically oxidized species in MeCN. λ_{max}, nm (ϵ, M⁻¹ cm⁻¹) 754 (4000), 548 sh (6900), 494 (7600), 362 (23 900), 316 sh (21 200). [h] λ_{max}, nm (ϵ, M⁻¹ cm⁻¹) 728 (2600), 530 (7200), 514 sh (7000), 360 (24 600), 312 sh (20 600).

---

(12) Vlček, A. A. *Coord. Chem. Rev.* **1982**, *43*, 39.

(13) Mukherjee, R. N.; Rajan, O. A.; Chakravorty, A. *Inorg. Chem.* **1982**, *21*, 785.

(14) The reaction occurs at room temperature (~300 K), but the use of boiling solvent is more convenient. Quite generally the stereochemistry of the product is unaffected by this temperature rise.

Table II. ^{1}H NMR Spectral Data

compd	^{1}H NMR[a,b], δ_{Me}
tc-[Ru(bpy)(tap)$_2$](ClO$_4$)$_2$·H$_2$O	2.16
cc-[Ru(bpy)(tap)$_2$](ClO$_4$)$_2$·H$_2$O	1.93, 2.21
tc-[Ru(en)(tap)$_2$](ClO$_4$)$_2$·H$_2$O	2.13[c]
mer-[Ru(tap)$_3$](ClO$_4$)$_2$·H$_2$O	2.05, 2.25
mer-[Ru(pap)(tap)$_2$](ClO$_4$)$_2$·H$_2$O	2.03, 2.18
tc-[Ru(acac)(tap)$_2$]ClO$_4$·H$_2$O	2.13[d]
tc-[Ru(Hto)(tap)$_2$]ClO$_4$·H$_2$O[e]	2.09, 2.11[f,g]

[a] Unless otherwise stated the solvent is (CD$_3$)$_2$SO, and SiMe$_4$ is used as internal standard. [b] Aromatic proton signals are not tabulated. [c] Chemical shift of CH$_2$ protons is 2.56 ppm. [d] δ_{Me} of acac is 1.96. [e] In CDCl$_3$. [f] δ_{Me} of Hto appears as a triplet at 1.08, 1.16, and 1.24 with J = 8 Hz. [g] δ_{CH_2} of Hto appears as a quartet at 3.96, 4.04, 4.10, and 4.18 with J = 8 Hz.

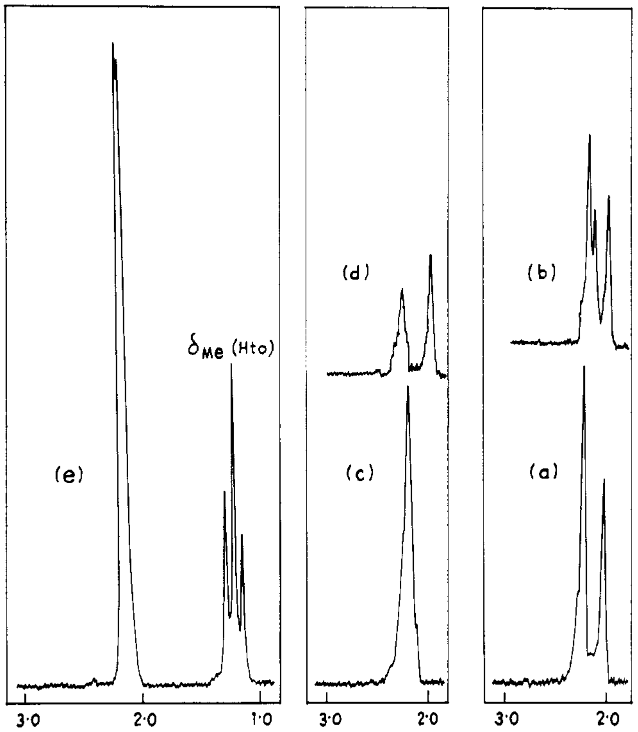

Figure 1. ^{1}H NMR methyl signals of tap in (a) *mer*-[Ru(tap)$_3$](ClO$_4$)$_2$·H$_2$O, (b) mixture of *mer*- and *fac*-[Ru(tap)$_3$](ClO$_4$)$_2$·H$_2$O, (c) *tc*-[Ru(bpy)(tap)$_2$](ClO$_4$)$_2$·H$_2$O, (d) *cc*-[Ru(bpy)(tap)$_2$](ClO$_4$)$_2$·H$_2$O, and (e) *tc*-[Ru(Hto)(tap)$_2$]ClO$_4$·H$_2$O. For (a) to (d) the solvent is Me$_2$SO-d_6 and for (e) it is CDCl$_3$.

(x = 1 or 2) obtained therefrom. Further, the mixed tris complex resulting from the reaction of bpy and *cc*-Ru(OH$_2$)$_2$(tap)$_2^{2+}$ (**3**) shows two equally intense methyl signals (Figure 1), demonstrating that here the RuL$_2$ group has the same symmetry as in **3**. Thus, the synthetic reaction 4 is stereoretentive (within the limits of ^{1}H NMR detection), i.e.

$$\mathbf{2} \xrightarrow{B} tc\text{-RuBL}_2{}^{x+} \qquad (5)$$

$$\mathbf{3} \xrightarrow{B} cc\text{-RuBL}_2{}^{x+} \qquad (6)$$

It is reasonable to assume that eq 5 and 6 apply for unsymmetrical bidentate ligands also. Here the two L ligands in RuBL$_2{}^{x+}$ become inherently nonequivalent, as observed in the cases of *tc*-Ru(pap)(tap)$_2^{2+}$ and *tc*-Ru(Hto)(tap)$_2^{+}$.

(b) Case of Ru(tap)$_3^{2+}$. The formation of the unmixed tris chelate Ru(tap)$_3^{2+}$ (reaction 7) is of special interest. Assuming stereoretentivity, *tc*-Ru(OH$_2$)$_2$(tap)$_2^{2+}$ should give rise exclusively to the meridional isomer (**4**). This isomer is of C_1 symmetry, and three different methyl signals are expected in principle. In the product[15] of reaction 7, two signals of relative

$$\text{Ru(OH}_2)_2(\text{tap})_2{}^{2+} + \text{tap} \xrightarrow{\text{MeOH}} \text{Ru(tap)}_3{}^{2+} \qquad (7)$$

intensity 1:2 are observed (Figure 1). This is not incompatible with structure **4** since meridional tris chelates are well documented[16] to display this type of behavior, i.e., two of the three rings becoming equivalent in practice.[17]

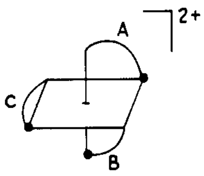

mer
4

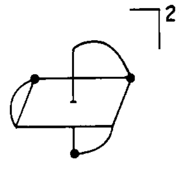

fac
5

Application of reaction 7 to *cc*-Ru(OH$_2$)$_2$(tap)$_2^{2+}$ should in principle produce both the meridional (**4**) and the facial (**5**) isomers of Ru(tap)$_3^{2+}$. If aquo displacement is purely statistical, the two isomers should form in equal amounts. However, crowding of three aryl rings in the facial isomer is likely to make it sterically unfavorable.[16] The product obtained by room-temperature synthesis shows the expected two signals of **4**, but a new signal (δ_{Me} 2.18) of relatively low intensity is also present (Figure 1). This signal is most probably due to **5**, and its low population is due to the steric factor. When the synthesis is carried out in boiling methanol, the signal for **5** becomes more pronounced (Figure 1). Attempted isomer separation on columns of alumina or silica gel has been vitiated by substrate decomposition.

Preliminary rate data have shown that reaction 4 as well as the solvolysis and anation of **2** proceed primarily by a dissociative mechanism, and this is not incompatible[18] with the observed stereochemistry. The substitution of[19] Me$_2$SO by PPh$_3$ in RuX$_2$(η-C$_6$H$_6$)(Me$_2$SO) and of[18] water by pyridines and nitriles in Ru(OH$_2$)(NH$_3$)$_5^{2+}$ is reported to be dissociative. In contrast, the displacement of chloride by tertiary phosphines in isomers of RuCl$_2$L$_2$ is associative and stereodynamic.[2b,11]

Electron-Transfer Properties. The metal oxidation and ligand reduction behavior of the complexes (reaction 2 and 3) have been studied by using cyclic voltammetry (CV) and differential pulse voltammetry (DPV) in acetonitrile (0.1 M TEAP). The potential range 0 to +2.4 V was scanned by using a platinum working electrode. For the region 0 to −2.7 V a hanging mercury drop electrode (HMDE) was utilized.[20] All potentials are referenced to a saturated calomel electrode (SCE). The DPV technique was particularly useful for observing metal oxidation and ligand reduction signals close to the solvet cutoff region. With the help of this technique we have been able to identify high metal oxidation potentials that others[6] have failed to observe.

(a) High Metal Oxidation Potentials. Quite generally the ruthenium(III)–ruthenium(II) couple occurs at high positive potentials[2–6,21,22] in complexes of RuL$_2^{2+}$; a formal potential

---

(15) This is true when the complex is synthesized at room temperature. When the synthesis is carried out in boiling methanol, an additional relatively weak methyl signal (δ_{Me} 2.18) appears, presumably due to formation of some facial isomer.

(16) Chakravorty, A.; Kalia, K. C. *Inorg. Chem.* **1967**, *6*, 690.

(17) The two equivalent rings are presumably[16] A and B (structure **5**), the unique ring being C. Note that by interchanging N^1 and N^2 in the C ring the meridional isomer is converted to the facial isomer. This does not happen in the cases of A and B rings. The C ring is different from rings A and B.

(18) Allen, R. J.; Ford, P. C. *Inorg. Chem.* **1972**, *11*, 679.

(19) Carr, C. M.; Davies, D. M.; Gower, M.; Kane-Maguire, L. A. P.; Sweigart, D. A. *J. Chem. Soc., Dalton Trans.* **1981**, 923.

(20) Studies were also made by using platinum as the working electrode down to the accessible limit, −1.7 V. Within this limit the results are virtually identical with those measured by using HMDE as the working electrode. With the HMDE the accessible range extends by nearly another volt.

Table III. Voltammetric Data[a-c] in Acetonitrile at 298 K

compd	$E°_{298}$ for metal-centered oxidn, V	$-E°_{298}$ for ligand-based redn, V
[Ru(pap)(bpy)$_2$](ClO$_4$)$_2$·H$_2$O	1.60[d]	0.52, 1.26, 1.81, 2.15, 2.53
[Ru(tap)(bpy)$_2$](ClO$_4$)$_2$·H$_2$O	1.60[d]	0.52, 1.26, 1.81, 2.13, 2.47
tc-[Ru(bpy)(pap)$_2$](ClO$_4$)$_2$·H$_2$O	1.88[d]	0.21, 0.72, 1.47, 1.75, 2.06, 2.44
tc-[Ru(bpy)(tap)$_2$](ClO$_4$)$_2$·H$_2$O	1.89[d]	0.21, 0.72, 1.48, 1.78, 2.11, 2.49
cc-[Ru(bpy)(tap)$_2$](ClO$_4$)$_2$·H$_2$O	1.92[d]	0.23, 0.61, 1.40, 1.52, 1.85, 2.19
tc-[Ru(en)(tap)$_2$](ClO$_4$)$_2$·H$_2$O	1.69	0.32, 0.93, 1.60, 1.80
mer-[Ru(pap)$_3$](ClO$_4$)$_2$·H$_2$O	2.10	0.13, 0.45, 0.94, 1.59, 1.92, 2.06
mer-[Ru(tap)(pap)$_2$](ClO$_4$)$_2$·H$_2$O	2.14	0.11, 0.43, 0.91, 1.57, 1.92, 2.04
mer-[Ru(pap)(tap)$_2$](ClO$_4$)$_2$·H$_2$O	2.19	0.08, 0.41, 0.91, 1.57, 1.93, 2.03
mer-[Ru(tap)$_3$](ClO$_4$)$_2$·H$_2$O	2.23	0.10, 0.43, 0.93, 1.59, 1.89, 1.95
tc-[Ru(acac)(tap)$_2$](ClO$_4$)·H$_2$O	1.34,[d] 1.99[d]	0.41, 0.98, 1.90
tc-[Ru(OMeto)(pap)$_2$](ClO$_4$)·H$_2$O	0.71[d]	0.54, 1.06, 1.89, 2.20
tc-[Ru(Meto)(pap)$_2$](ClO$_4$)·H$_2$O[e]	0.78[d]	0.53, 1.06, 1.91, 2.21
tc-[Ru(Hto)(pap)$_2$](ClO$_4$)·H$_2$O	0.82[d]	0.48, 0.97, 1.82, 2.20
tc-[Ru(Clto)(pap)$_2$](ClO$_4$)·H$_2$O	0.84[d]	0.48, 0.97, 1.78, 2.16
tc-[Ru(CO$_2$Etto)(pap)$_2$](ClO$_4$)·H$_2$O[f]	0.89[d]	0.42, 0.94, 1.71, 2.14
tc-[Ru(NO$_2$to)(pap)$_2$](ClO$_4$)·H$_2$O	0.93[d]	0.41, 0.93, 1.69, 2.11
tc-[Ru(Hto)(tap)$_2$](ClO$_4$)·H$_2$O	0.81	0.49, 0.97, 1.83, 2.20

[a] Meaning and units of symbols are the same as in text. [b] Supporting electrolyte TEAP (0.1 M); solute concentration ~10^{-3} M. [c] Unless otherwise stated the $E°_{298}$'s are from DPV data; scan rate is 10 mV s^{-1}; modulation amplitude (ΔE) is 25 mV; $E°_{298} = E_p + 0.5(\Delta E)$, where E_p is DPV peak potential. [d] Cyclic voltammetric data: scan rate, 50 mV s^{-1}; $E°_{298} = 0.5(E_{pc} + E_{pa})$, where E_{pc} and E_{pa} cathodic and anodic peak potentials, respectively. [e] 4.56 mg of complex exhaustively oxidized at +1.2 V. Q: calcd, 0.58 C; found, 0.62 C. [f] 4.1 mg of complex oxidized at +1.2 V. Q: calcd, 0.48 C; found, 0.53 C.

value as high as 2.08 V is observed[2b] in a phosphine complex. Values higher than this are now reported for some of the tris complexes (Table III, Figure 2). The general redox couple is 8. The one-electron stoichiometry of the couple 8 is es-

$$\mathrm{Ru^{III}BL_2}^{(x+1)+} + e^- \rightleftharpoons \mathrm{Ru^{II}BL_2}^{x+} \qquad (8)$$

tablished from consideration of current height data.[23] Attempted constant potential coulometry at the required high potentials gave continuous counts in most cases. However, some triazene 1-oxide species such as Ru(Meto)(pap)$_2^+$ and

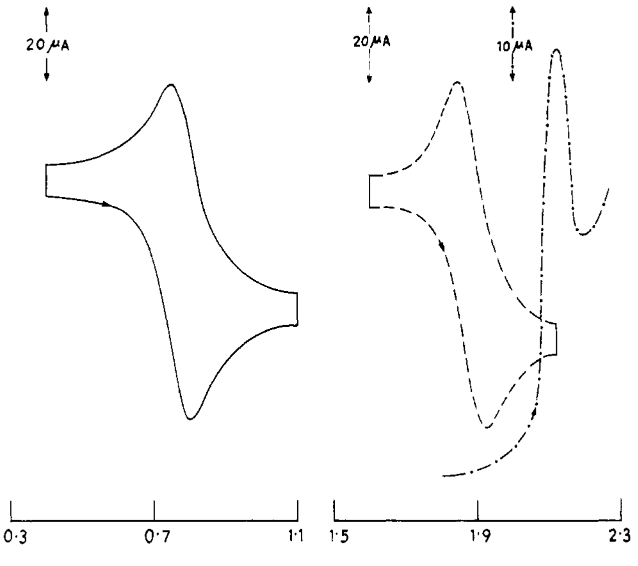

Figure 2. Cyclic voltammograms (scan rate 50 mV s^{-1}) of (a) *tc*-[Ru(Meto)(pap)$_2$]ClO$_4$·H$_2$O (—) and (b) *tc*-[Ru(bpy)(pap)$_2$](ClO$_4$)$_2$·H$_2$O (- - -). Differential pulse voltammogram (scan rate 10 mV s^{-1} and modulation amplitude 25 mV) of (c) *mer*-[Ru(pap)$_3$](ClO$_4$)$_2$·H$_2$O (·····). In all cases the solvent is acetonitrile (0.1 M TEAP) and the electrode is platinum.

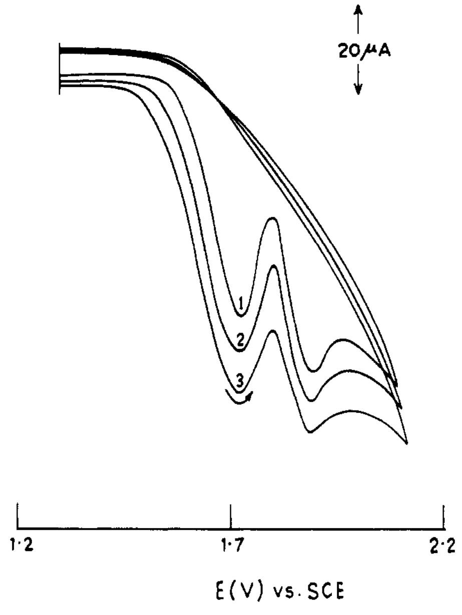

Figure 3. Cyclic voltammograms of *tc*-[Ru(en)(tap)$_2$](ClO$_4$)$_2$·H$_2$O in acetonitrile (0.1 M TEAP) at platinum electrode. Scan rates (mV s^{-1}): (1) 50, (2) 100, (3) 200.

Ru(CO$_2$Etto)(pap)$_2^+$ could be exhaustively electrolyzed at +1.20 V, confirming the one-electron stoichiometry (Table III). In each case the oxidized complex (bronze color) is sufficiently stable in the electrolyzed solution for spectral examination. The most characteristic feature is an allowed low-energy band (~740 nm, Table I) assignable to[24] RtO → Ru^{III} charge transfer.

In addition to couple 8 at +1.34 V, Ru(acac)(tap)$_2^+$ shows a second quasireversible electrode reaction near 2 V. It is reasonable[25-27] to assign this to the ruthenium(IV)–rutheni-

---

(21) Using electrochemical data, Chatt has proposed[22] a set of ligand constants, P_L, for several ligands. Much of the available ruthenium(III)–ruthenium(II) data[2,3,6] for complexes of type RuL$_2$YZ^{p+} (where Y and Z are halide, pseudohalide, hydroxide ion, phosphines, and nitriles; the cases Y = Z and Y ≠ Z are both included) correlate with P_L values. In some cases the fit is poor, e.g., *tc*-Ru(OH)$_2$L$_2$. Using the above $E°_{298} - P_L$ line and experimental $E°_{298}$ of bidentate ligands used by us, we found their P_L values to be Rto −2.84, acac −1.94, en −1.32, bpy −0.99, and pap −0.61. The high P_L value of pap corresponds to the observed high $E°_{298}$.

(22) Chatt, J. *Coord. Chem. Rev.* **1982**, *43*, 337.

(23) The 1e$^-$ nature of each couple is established beyond doubt by comparison of current heights with those of the standard ruthenium(III)–ruthenium(II) couple, e.g., in RuCl$_2$L$_2$, where coulometric data are also available.[2a]

(24) Mukherjee, R. N.; Chakravorty, A. *J. Chem. Soc., Dalton Trans.* **1983**, 955.

(25) Formal potentials of some other ruthenium(IV)–ruthenium(III) couples are *tc*-Ru(OH)(OH$_2$)(pap)$_2^+$ 1.89,[3] *tc*-Ru(OH)$_2$(pap)$_2$ 1.53,[3] Ru(acac)(bpy)$_2^+$ 1.82 (E_{pa}),[26] RuCl$_2$(bpy)$_2$ 1.98 V.[27]

Table IV. Selected Bond Distances and Formal Potentials of Some Ruthenium(II) Complexes

compd	Ru-N, Å	$E°_{298}$- (Ru(III)-Ru(II)),[a] V
$RuCl_2(bpy)_2$	2.06[b]	0.30
$RuCl_2(pap)_2$	2.05[c] 1.98[d]	1.05,[e] 1.10[f]
$RuCl_2(HA)_2$	1.98[g]	1.20

[a] All measurements are made cyclic voltammetrically in acetonitrile (0.1 M TEAP) by using platinum as the working electrode at 298 K. [b] Estimated from Ru-N distance of $Ru(bpy)_3^{2+}$ (ref 33). [c] Average Ru-N^1; the distances in the *tc* and *cc* isomers lie within ±0.01 Å (ref 3, 10). [d] Average Ru-N^2; the distances in the *tc* and *cc* isomers lie within ±0.01 Å (ref 3, 10). [e] *tc* isomer. [f] *cc* isomer. [g] All the Ru-N distances lie within the range 1.98 ± 0.01 Å (ref 32).

um(III) couple. The $Ru(en)(tap)_2^{2+}$ complex also displays two oxidative responses. These are very closely spaced, and in cyclic voltammetry the corresponding cathodic responses are not observed at all (Figure 3). The peak at lower potential is no doubt due to the oxidative part of the couple 8. The response at higher potential most probably represents the ruthenium(II) → ruthenium(III) oxidation of an α-diimine analogue of $Ru(en)(tap)_2^{2+}$ formed by secondary chemical transformation of electrogenerated $Ru(en)(tap)_2^{3+}$. This type of behavior is well documented in $Ru(bpy)_3^{2+}$ chemistry.[28-31]

(b) Bond Distance and Formal Potential. In the series $Ru(bpy)_3^{2+}$ ($E°_{298}$ = 1.29 V), $Ru(bpy)_2L^{2+}$, $Ru(bpy)L_2^{2+}$, and RuL_3^{2+}, the replacement of each bpy by L lead to a monotonic increase of $E°_{298}$ by ~300 mV. In this context we wish to note here that a qualitative correlation between Ru-N bond distance and ruthenium(III)-ruthenium(II) formal potentials (Table IV) exists in a group of complexes of type $RuCl_2$(bidentate)$_2$, where the bidentate π-acceptor ligand is bpy, L, or (phenylazo)benzaldoxime (HA).[32] The Ru-N bond distance in *cis*-$RuCl_2(bpy)_2$ is not known, but it is reasonable to assume it to be ~2.06 Å as in[33] $Ru(bpy)_3^{2+}$. In the *tc* and *cc* isomers[3,10] of $RuCl_2(pap)_2$, the Ru-N^1 distance is nearly equal to the Ru-N distance in the bpy complex; the Ru-N^2 distance is however much shorter. Clearly the azo nitrogen binds ruthenium(II) more strongly than the pyridine nitrogen. That ruthenium-azo π-bonding plays a role here is also evident in the long N-N distance (1.30 ± 0.02 Å)[3,10] and in lowered[2b,3,5,6] N=N stretching frequencies (Table I). Examination of Table IV clearly shows that $E°_{298}$ increases as the average Ru-N bond distance decreases (increased π-bonding). Thus, the stronger the Ru-N bond, the higher is the potential required to oxidize the metal—a result in consonance with principles of redox thermodynamics.[13] It is tempting to suggest that the greater stability of the t_2 level associated with a short Ru-N bond is responsible for higher $E°_{298}$ values. Such an approach is, however, subject to caution since redox potentials depend on a number of factors of which d-orbital splitting is often not the most important.[13] To restate our conclusion: the short Ru-N^2 bond (which makes the average Ru-N distance also short) presumably arising from strong Ru-azo π-bonding is reflected in the high $E°_{298}$ values of Ru-L complexes.

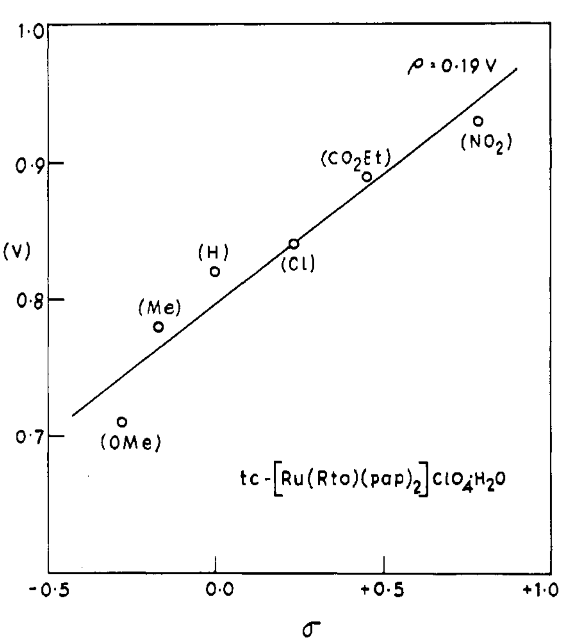

Figure 4. Linear least-squares fit of $E°_{298}$ vs. σ for *tc*-$[Ru(Rto)(pap)_2]ClO_4 \cdot H_2O$.

(c) Substituent Effect. The six triazene 1-oxide complexes (6) provide an opportunity for examining the polar effect of

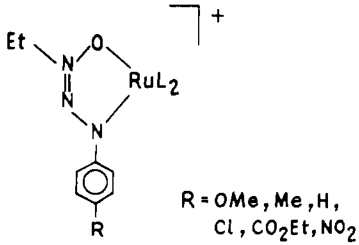

6

remote substituents on couple 8. The value progressively increases as R becomes more and more electron withdrawing. The plot of $E°_{298}$ vs. Hammett substituent constant (σ) is excellently linear (Figure 4) with a reaction constant (ρ) of 0.19 V. The latter value is close to those observed[13,24] in the one-electron reduction of $Fe(Rto)_3$, $Co(Rto)_3$, $Ru(Rto)_3$, and $Cu(Rto)_2$.

(d) Ligand Reduction: Complete Electron-Transfer Series. Cursory reports on the reduction of Ru(II)L complexes at negative potentials have appeared.[2-6] A systematic examination of the observed processes are made here. The free ligand pap displays two quasireversible cyclic voltammetric responses with peak-to-peak separation in the range 120-150 mV. Since no other reduction is observed, the nondegenerate LUMO is well separated from the next higher UMO. On comparison of potentials of couples 9 and 10 with those of

$$\text{pap} + e^- \rightleftharpoons \text{pap}^- \qquad E°_{298} = -1.31 \text{ V} \qquad (9)$$

$$\text{pap}^- + e^- \rightleftharpoons \text{pap}^{2-} \qquad E°_{298} = -1.57 \text{ V} \qquad (10)$$

bpy[34] on the one hand and aromatic azo ligands[35] on the other, it emerges that the electron-accepting LUMO of pap is pri-

---

(26) Mukherjee, R. N.; Chakravorty, A., unpublished results.

(27) Weaver, T. R.; Meyer, T. J.; Adeyemi, S. A.; Brown, G. M.; Eckberg, R. P.; Hatfield, W. E.; Johnson, E. C.; Murray, R. W.; Untereker, D. *J. Am. Chem. Soc.* **1975**, *97*, 3039.

(28) Brown, G. M.; Weaver, T. R.; Keene, F. R.; Meyer, T. J. *Inorg. Chem.* **1976**, *15*, 190.

(29) Keene, F. R.; Salmon, D. J.; Meyer, T. J. *J. Am. Chem. Soc.* **1976**, *98*, 1884.

(30) Adcock, P. A.; Keene, F. R. *J. Am. Chem. Soc.* **1981**, *103*, 6494. Ridd, M. J.; Keene, F. R. *Ibid.* **1981**, *103*, 5733.

(31) The $Ru(en)(bpy)_2^{3+}$-$Ru(en)(bpy)_2^{2+}$ couple ($E°_{298}$ = 0.96 V)[28] is nearly reversible in the cyclic voltammetric time scale, but left to itself the ruthenium(III) complex is unstable and eventually affords the α-diimine chelate $Ru(NH{=}CHCH{=}NH)(bpy)_2^{2+}$. In the tap complex, ruthenium(III)-ruthenium(II) $E°_{298}$ is much higher, and consequently the reaction succeeding the electrochemical formation of $Ru^{III}(en)(tap)_2^{3+}$ is expected to be faster. The electrochemical behavior of $Ru(en)(tap)_2^{2+}$ is closely analogous[28] to that of $Ru(2\text{-}H_2NCH_2py)(bpy)_2^{2+}$.

(32) Chakravarty, A. R.; Chakravorty, A.; Cotton, F. A.; Falvello, L. R.; Ghosh, B. K.; Tomas, M. *Inorg. Chem.* **1983**, *22*, 1897.

(33) Rillema, D. P.; Jones, D. S.; Levy, H. A. *J. Chem. Soc., Chem. Commun.* **1979**, 849.

(34) Kahl, J. L.; Hanck, K. W.; DeArmond, K. *J. Phys. Chem.* **1978**, *82*, 540.

(35) Sadler, J. L.; Bard, A. J. *J. Am. Chem. Soc.* **1968**, *90*, 1979.

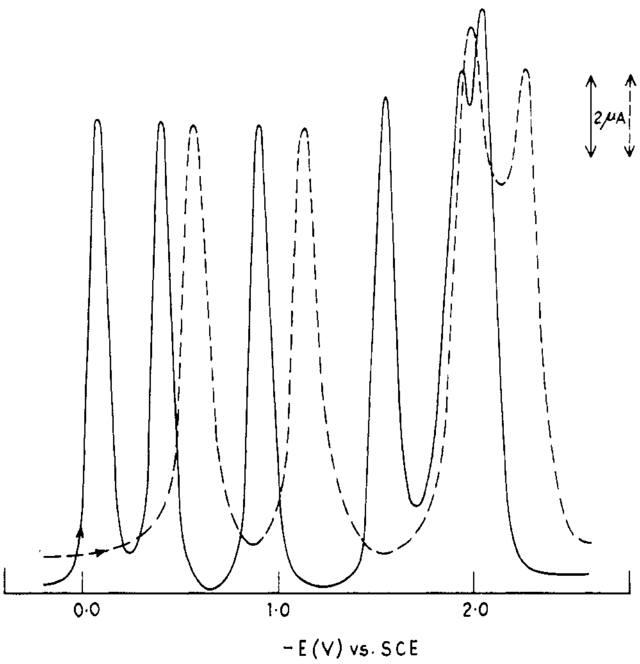

Figure 5. Differential pulse voltammograms in acetonitrile (0.1 M TEAP) at hanging mercury drop electrode (scan rate 10 mV s^{-1}, modulation amplitude 25 mV): *mer*-[Ru(pap)(tap)$_2$](ClO$_4$)$_2$·H$_2$O (—); *tc*-[Ru(Meto)(pap)$_2$]ClO$_4$·H$_2$O (- - -).

marily azo in character and couples 9 and 10 essentially correspond to processes 11 and 12, respectively.

$$-\mathrm{N}{=}\mathrm{N}- + e^- \rightleftharpoons -\mathrm{N}\underset{\cdot\cdot}{-}\mathrm{N}-^{-} \qquad (11)$$

$$-\mathrm{N}\underset{\cdot\cdot}{-}\mathrm{N}-^{-} + e^- \rightleftharpoons -\mathrm{N}-\mathrm{N}-^{2-} \qquad (12)$$

Data for the tris complexes are in Table III. Successive one-electron reductions are quite generally observed. Due to the positive charge of the metal ion, the formal potential for the first reduction of L in ruthenium complexes is uniformly more positive than that of free L.

In RuL_3^{2+} the three LUMO's of L would combine to produce three closely spaced orbitals.[36] Six successive reductions[37] could thus occur in principle. All of them are actually observed in careful[38] DPV experiments (Figure 5). In the cases of $Ru(en)L_2^{2+}$ and $Ru(Rto)L_2^{+}$, the four possible L-based reductions are experimentally identifiable.

The observation of a complete set of six reductions in the tris chelate is rare. Like L, bpy also has one electrochemically accessible LUMO, but in $Ru(bpy)_3^{2+}$ only four of the six reductions are observable.[34,39–41] Each reduction potential of $Ru(bpy)_3^{2+}$ is more negative than the corresponding potential of RuL_3^{2+} (the same holds for the free ligands). It is therefore of interest to examine the behavior of mixed bpy–L complexes. In $Ru(bpy)L_2^{2+}$, all the six reductions are observed, but in $Ru(bpy)_2L^{2+}$, the last one is inaccessible. The successive reduction potentials of a group of compounds are graphically represented in Figure 6. Indications[42] are strong that in the

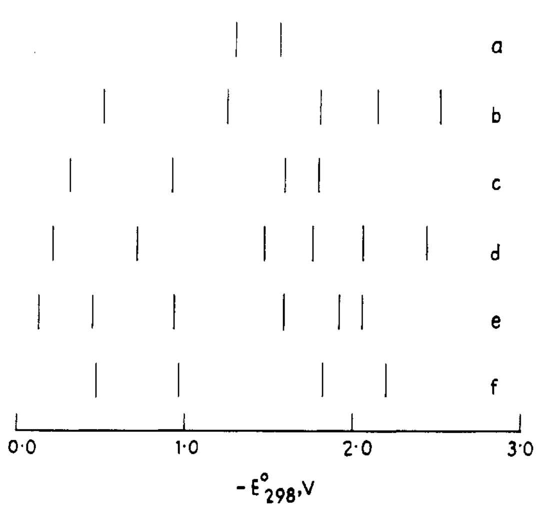

Figure 6. Formal ligand reduction potentials of (a) pap, (b) [Ru(pap)(bpy)$_2$](ClO$_4$)$_2$·H$_2$O, (c) *tc*-[Ru(en)(tap)$_2$](ClO$_4$)$_2$·H$_2$O, (d) *tc*-[Ru(bpy)(pap)$_2$](ClO$_4$)$_2$·H$_2$O, (e) *mer*-[Ru(pap)$_3$](ClO$_4$)$_2$·H$_2$O, and (f) *tc*-[Ru(Meto)(pap)$_2$]ClO$_4$·H$_2$O.

Table V. Spectroelectrochemical Data[a]

complex[b]	ΔE,[c] V	ν_{MLCT}, cm^{-1} calcd[d]	obsd	ref
tc-[Ru(Ph$_2$P(CH$_2$)$_3$PPh$_2$)(pap)$_2$]$^{2+}$	2.25	21 150	20 490	2b
tc-[Ru(PPh$_2$Me)Cl(tap)$_2$]$^+$	2.06	19 610	18 730	2b
tc-[Ru(Ph$_2$PMe)Br(pap)$_2$]$^+$	1.89	18 240	18 870	2b
mer-[Ru(pap)$_3$]$^{2+}$	2.23	20 990	20 330	this work
[Ru(pap)(bpy)$_2$]$^{2+}$	2.12	20 100	20 240	2a
tc-[Ru(bpy)(tap)$_2$]$^{2+}$	2.10	19 940	19 530	this work
[Ru(btz)(pap)$_2$]$^{2+}$	2.23	20 990	19 420	6
tc-[Ru(py)(MeCN)(pap)$_2$]$^{2+}$	2.20	20 740	19 610	3
tc-[Ru(OH)(OH$_2$)(pap)$_2$]$^+$	1.76	17 190	18 180	3
tt-[RuCl$_2$(tap)$_2$]	1.64	16 230	15 770	2a
tt-[RuBr$_2$(tap)$_2$]	1.62	16 070	15 750	2a
tt-[RuI$_2$(tap)$_2$]	1.64	16 230	15 600	2a
[RuBr$_2$(pap)$_2$]	1.73[e]	16 950	16 950[e]	6
tc-[Ru(en)(tap)$_2$]$^{2+}$	2.01	19 210	18 590	this work
tc-[Ru(acac)(tap)$_2$]$^+$	1.75	17 110	17 730	this work
tc-[Ru(Hhydxm)(pap)$_2$]$^+$	1.49	15 020	14 930	43
[Ru(N$_3$)$_2$(pap)$_2$]	1.48[e]	14 940	16 260[e]	6
[Ru(tu)$_2$(pap)$_2$]$^{2+}$	1.46	14 780	17 090	6
tc-[Ru(Meto)(pap)$_2$]$^+$	1.31	13 570	13 740	this work
tc-[Ru(hydxm)(pap)$_2$]	1.03	11 310	11 980	43

[a] Unless otherwise stated the electrochemical and spectral data are in acetonitrile. [b] Abbreviations: btz, 4,4′-bithiazole; Hhydxm, benzohydroxamic acid; tu, thiourea. [c] Meaning is as in eq 14 of text. [d] Calculated by using eq 13 of text. [e] In dichloromethane.

---

(36) Due to lack of symmetry (trans structure) each level is in principle nondegenerate.

(37) The spin multiplicities of the various reduced species are not known. However, in view of the small differences between successive reduction potentials it is reasonable to assume that the electrons are added successively to L ligands retaining a high-spin configuration:

$$[RuL_3]^{2+} \xrightarrow{1} [Ru(L\cdot)L_2]^+ \xrightarrow{2} [Ru(L\cdot)_2L] \xrightarrow{3} [Ru(L\cdot)_3]^- \xrightarrow{4}$$
$$[Ru(L{:})(L\cdot)_2]^{2-} \xrightarrow{5} [Ru(L{:})_2(L\cdot)]^{3-} \xrightarrow{6} [Ru(L{:})_3]^{4-}$$

It is significant that $|E°_{298}(1) - E°_{298}(2)| > |E°_{298}(2) - E°_{298}(3)|$. Further, $|E°_{298}(3) - E°_{298}(4)|$ is considerably greater than the difference in the formal potentials of couples 9 and 10. The latter result suggests that the redox orbitals may be of relatively localized nature.[12]

(38) It is essential to use anhydrous solvent to be able to observe all six reductions. Presence of trace moisture leads to the collapse of the fifth and sixth reduction responses into a single two-electron process evidently due to protonation of the reduced species.

(39) Tokel-Takvoryan, N. E.; Hemingway, R. E.; Bard, A. J. *J. Am. Chem. Soc.* **1973**, *95*, 6582.

(40) By incorporating electron-withdrawing substituents on bpy it is possible[41] to bring all reductions within the accessible range. In $Ir(bpy)_3^{3+}$ all the six reductions are observed.[34]

(41) Elliott, C. M. *J. Chem. Soc., Chem. Commun.* **1980**, 261.

(42) This proposal is based on consideration of (i) the behavior of four reduction potentials of $Ru(bpy)L_2^{2+}$ and $Ru(en)L_2^{2+}$, (ii) the near equality of the difference $E°_{298}(1) - E°_{298}(2)$ in $Ru(bpy)_2L^{2+}$ with the difference $E°_{298}(2) - E°_{298}(3)$ in $Ru(en)L_2^{2+}$ and $Ru(bpy)L_2^{2+}$ and the difference $E°_{298}(3) - E°_{298}(4)$ of RuL_3^{2+} (where $E°_{298}(1)$ is the reduction at highest potential (see text), $E°_{298}(2)$ is the reduction at the next level, and so on). Admittedly the proposal is not a unique rationalization of the experimental results. It however appears to be a plausible one.

bpy–L mixed complexes the L ligand(s) is (are) completely reduced ($L \rightarrow L^{-\cdot} \rightarrow L^{-}:$) before bpy reduction occurs.

(e) Spectroelectrochemical Correlation. With the present results, we now have at hand ruthenium(III)–ruthenium(II) and ligand reduction potentials for a sizeable group of Ru–L complexes.[2–6,43] The energy of the MLCT band is also available in each case. With the representative data of Table V we wish to note here that the energy of the MLCT band is predictable to within ±1000 cm^{-1} in virtually all the reported cases with the help of eq 13. Here $E^\circ_{298}(Ru)$ is the formal

$$\nu_{MLCT} = 8065(\Delta E^\circ) + 3000 \qquad (13)$$

$$\Delta E^\circ = E^\circ_{298}(Ru) - E^\circ_{298}(L) \qquad (14)$$

potential (in V) of the ruthenium(III)–ruthenium(II) couple, $E^\circ_{298}(L)$ is that of the first (the one occurring at the highest potential) L-reduction couple, and ν_{MLCT} is the frequency of the charge-transfer band in cm^{-1}. The factor 8065 is used to convert V to cm^{-1} and the term 3000 cm^{-1} is of empirical origin. The observed range of $E^\circ_{298}(Ru)$ is 2.2 to 0.4 V and that of $E^\circ_{298}(L)$ is –0.1 to –0.7 V. The resultant range of ΔE° is 2.3–1 V. The observed MLCT energies lie in the interval 12 000–21 000 cm^{-1}. The ranges covered by this correlation are thus quite wide. The significance of this result will be reported in due course in the broader context of ruthenium complexes of unsaturated ligands in general. Indications are strong that a single linear equation can be devised to connect ν_{MLCT} and ΔE° in a variety of ruthenium complexes, including those of L.

Concluding Remarks. It is demonstrated that the isomerically pure tris chelates of type $RuBL_2^{x+}$ are formed by stereoretentive displacement of water from $Ru(OH_2)_2L_2^{2+}$. We wish to add that in this reaction, *tc*- or *cc*-$RuCl_2L_2$ can be utilized as a bidentate ligand (reaction 15). The chemistry

$$Ru(OH_2)_2L_2^{2+} + RuCl_2L_2 \rightarrow L_2Ru(\mu\text{-}Cl)_2RuL_2^{2+} + 2H_2O \qquad (15)$$

of the resulting dinuclear complex and related species is under investigation.

Highly positive metal oxidation potentials have been identified. The potentials of the RuL_3^{2+} complexes are indeed the highest among all reported ruthenium(III)–ruthenium(II) potentials. The role of Ru–N^2 π-bonding is noted with the help of bond distance data. Complete ligand-based electron-transfer series are observed in several cases. With the help of metal oxidation and ligand reduction potentials, it has been found feasible to predict the energy of MLCT transition to a good degree of approximation.

Experimental Section

Materials. The isomeric $[Ru(OH_2)_2L_2](ClO_4)_2 \cdot H_2O$ complexes and species of type $[RuL(bpy)_2](ClO_4)_2 \cdot H_2O$ were prepared by using reported methods.[2a,3] The ligand L was synthesized as reported previously.[2a,7] The triazene 1-oxides (HRto) were prepared as before.[13] Dinitrogen was purified by bubbling it through an alkaline dithionite reducing solution. The purification/preparation of solvent and supporting electrolyte for electrochemical work was done as before.[13] All other chemicals and organic solvents used for preparative work were of reagent grade and were used without further purification.

Measurements. Spectroscopic data were obtained by using the following instruments: electronic spectra, Cary 17D or Pye Unicam SP8-150 spectrophotometer; IR spectra (KBr disk, 4000–400 cm^{-1}), Beckman IR-20A spectrophotometer; ^1H NMR spectra, Varian T-60A or Jeol FX-100 spectrometer. Solution electrical conductivity was measured with a Philips PR 9500 bridge with a solute concentration of $\sim 10^{-3}$ M. Voltammetric measurements were done by using a PAR Model 370-4 electrochemistry system: 174A, polarographic analyzer; 175, universal programmer; RE0074, XY recorder. All experiments were done under dinitrogen atmosphere in a three-electrode configuration by using either a planar Beckman Model 39273 platinum electrode or a Metrohm E410 hanging mercury drop electrode as the working electrode. All results were collected at 298 K and are referenced to a saturated calomel electrode (SCE). The reported potentials are uncorrected for junction contribution. Controlled potential coulometry required the PAR 173 potentiostat, PAR 179 digital coulometer, and a PAR 377A cell system.

The following σ values for para substituents were used:[13,24] OMe, –0.27; Me, –0.17; H, 0.00; Cl, +0.23; CO_2Et, +0.45; NO_2 +0.78.

Preparation of Complexes. *tc*-(Bipyridine)bis[2-(phenylazo)pyridine]ruthenium(II) Perchlorate Monohydrate, *tc*-$[Ru(bpy)(pap)_2](ClO_4)_2 \cdot H_2O$. To a solution of 200 mg (0.27 mmol) of *tc*-$[Ru(OH_2)_2(pap)_2](ClO_4)_2 \cdot H_2O$ in 15 mL of methanol was added 65 mg (0.42 mmol) of bpy. The mixture was then heated to reflux for 1 h. The blue-violet solution gradually turned red. To the hot solution was added 250 mg of sodium perchlorate, and the mixture was then kept in the refrigerator for 12 h. Almost quantitative precipitation occurred. The precipitate was collected by filtration and washed thoroughly with water and methanol. It was recrystallized from methanol. The dark colored needle-shaped crystals were collected by filtration and dried in vacuum over P_4O_{10}. The yield was 70%.

The tap analogues of *tc* and *cc* isomers were prepared by using the same reaction stoichiometry and conditions starting with *tc*-$[Ru(OH_2)_2(tap)_2](ClO_4)_2 \cdot H_2O$ and *cc*-$[Ru(OH_2)_2(tap)_2](ClO_4)_2 \cdot H_2O$, respectively. The yields were 75% and 65%, respectively.

***tc*-(Ethylenediamine)bis[2-(*m*-tolylazo)pyridine]ruthenium(II) Perchlorate Monohydrate, *tc*-$[Ru(en)(tap)_2](ClO_4)_2 \cdot H_2O$.** To a methanolic solution (15 mL) of 200 mg (0.26 mmol) of *tc*-$Ru(OH_2)_2(tap)_2(ClO_4)_2 \cdot H_2O$ was added 25 mg (0.42 mmol) of en. Immediately the color of the solution turned blue. The resulting mixture was then heated to reflux for 1.5 h. The solution gradually turned red-violet. The cooled solution was then poured with stirring into 15 mL of water containing 1 g of sodium perchlorate. Immediately precipitate started depositing. This was collected by filtration and washed thoroughly with water. Recrystallization of the precipitate from 2:1 methanol–water mixture yielded dark colored crystals. The yield was 50%.

***mer*-Tris[2-(phenylazo)pyridine]ruthenium(II) Perchlorate Monohydrate, *mer*-$[Ru(pap)_3](ClO_4)_2 \cdot H_2O$.** pap (75 mg, 0.41 mmol) was added to a methanolic solution (15 mL) of 200 mg (0.27 mmol) of *tc*-$[Ru(OH_2)_2(pap)_2](ClO_4)_2 \cdot H_2O$. The mixture was stirred at room temperature for 6 h. The blue-violet solution gradually turned oprange. Sodium perchlorate (250 mg) was then added to the solution, and the mixture was again stirred for 15 min. Crystals started depositing. The mixture was kept in the refrigerator for 12 h for complete precipitation. The brown precipitate thus formed was collected by filtration and was washed thoroughly with water and finally with methanol. The precipitate was then recrystallized from methanol and the product was dried in vacuum over P_4O_{10}. The yield was 80%.

mer-$[Ru(tap)_3](ClO_4)_2 \cdot H_2O$, *mer*-$[Ru(tap)(pap)_2](ClO_4)_2 \cdot H_2O$, and *mer*-$[Ru(pap)(tap)_2](ClO_4)_2 \cdot H_2O$ were prepared similarly by using appropriate *tc*-$[Ru(OH_2)_2L_2](ClO_4)_2 \cdot H_2O$ and L. The yields were as follows: *mer*-$[Ru(tap)_3](ClO_4)_2 \cdot H_2O$, 80%; *mer*-$[Ru(tap)(pap)_2](ClO_4)_2 \cdot H_2O$, 75%; *mer*-$[Ru(pap)(tap)_2](ClO_4)_2 \cdot H_2O$, 80%.

The *cc*-$[Ru(OH_2)_2(tap)_2](ClO_4)_2 \cdot H_2O$ complex was similarly converted to the tris complex $[Ru(tap)_3](ClO_4)_2 \cdot H_2O$ (a mixture of *mer* and *fac* isomers; see text).

***tc*-(Acetylacetonato)bis[2-(*m*-tolylazo)pyridine]ruthenium(II) Perchlorate Monohydrate, *tc*-$[Ru(acac)(tap)_2](ClO_4) \cdot H_2O$.** Acetylacetone (40 mg, 0.40 mmol) was added to a 2:1 methanol–water (15 mL) solution of 200 mg (0.26 mmol) of *tc*-$[Ru(OH_2)_2(tap)_2](ClO_4)_2 \cdot H_2O$. The mixture was heated to reflux for 1.5 h in the presence of 500 mg of sodium carbonate and 250 mg of sodium perchlorate. A bright blue-violet solution thus resulted. The solution was then allowed to cool to room temperature, at which time shining crystals with copper sheen started depositing. The mixture was kept in the refrigerator for 12 h for complete precipitation. The precipitate was then collected by filtration, washed thoroughly with water, and dried under vacuum over P_4O_{10}. The yield was 75%.

***tc*-(Triazene 1-oxidato)bis[2-(phenylazo)pyridine]ruthenium(II) Perchlorate Monohydrate, *tc*-$[Ru(Rto)(pap)_2](ClO_4) \cdot H_2O$.** All the six complexes were prepared by using similar procedures. Details are therefore given for a representative member of the group.

***tc*-$[Ru(Clto)(pap)_2](ClO_4) \cdot H_2O$.** Nitrogen gas was passed for 15 min through a blue-violet solution of 200 mg (0.27 mmol) of *tc*-$[Ru(OH_2)_2(pap)_2](ClO_4)_2 \cdot H_2O$ in 15 mL of methanol. Then 1-ethyl-3-*p*-chlorophenyltriazene 1-oxide (75 mg, 0.54 mmol) and 100

---

(43) Ghosh, P.; Chakravorty, A., unpublished work.

mg of sodium carbonate was added, and the mixture was heated to reflux under dinitrogen atmosphere for 2 h. The reaction mixture was allowed to cool to room temperature. After evaporation of the solution to ~5 mL, red-violet crystals started depositing. It was then kept in the refrigerator for 12 h. The precipitate was collected by filtration and washed thoroughly with ice-cold water and finally with diethyl ether. The precipitates were dried under vacuum over P_4O_{10}. The yield was 50%.

***tc*-[Ru(Hto)(tap)$_2$](ClO$_4$)·H$_2$O** was similarly prepared starting from *tc*-[Ru(OH$_2$)$_2$(tap)$_2$](ClO$_4$)$_2$·H$_2$O and HHto.

Registry No. **6**$^+$ClO$_4^-$ (L = pap, R = OMe), 86646-05-1; **6**$^+$ClO$_4^-$ (L = pap, R = Me), 86646-07-3; **6**$^+$ClO$_4^-$ (L = pap, R = H), 86646-09-5; **6**$^+$ClO$_4^-$ (L = pap, R = Cl), 86646-11-9; **6**$^+$ClO$_4^-$ (L = pap, R = CO$_2$Et), 86646-13-1; **6**$^+$ClO$_4^-$ (L = pap, R = NO$_2$), 86646-15-3; **6**$^+$ClO$_4^-$ (L = tap, R = H), 86646-17-5; **6**$^{2+}$ (L = pap, R = Me), 86646-18-6; **6**$^{2+}$ (L = pap, R = CO$_2$Et), 86668-07-7; *tc*-[Ru(bpy)(pap)$_2$](ClO$_4$)$_2$, 86645-93-4; *tc*-[Ru(bpy)(tap)$_2$](ClO$_4$)$_2$, 86645-95-6; *cc*-[Ru(bpy)(tap)$_2$](ClO$_4$)$_2$, 86707-54-2; *tc*-[Ru(en)(tap)$_2$](ClO$_4$)$_2$, 86668-04-4; *mer*-[Ru(pap)$_3$](ClO$_4$)$_2$, 86645-97-8; *mer*-[Ru(tap)$_3$](ClO$_4$)$_2$, 86645-99-0; [Ru(tap)(pap)$_2$](ClO$_4$)$_2$, 86646-01-7; [Ru(pap)(tap)$_2$](ClO$_4$)$_2$, 86646-03-9; *tc*-[Ru(acac)(tap)$_2$](ClO$_4$), 86668-06-6; *fac*-[Ru(tap)$_3$](ClO$_4$)$_2$, 86707-56-4; *tc*-[Ru(OH$_2$)$_2$(pap)$_2$](ClO$_4$)$_2$, 84027-70-3; *tc*-[Ru(OH$_2$)$_2$(tap)$_2$](ClO$_4$)$_2$, 84027-73-6; *cc*-[Ru(OH$_2$)$_2$(tap)$_2$](ClO$_4$)$_2$, 84049-25-2; [Ru(pap)(bpy)$_2$](ClO$_4$)$_2$, 77321-13-2; [Ru(tap)(bpy)$_2$](ClO$_4$)$_2$, 77321-15-4.

Contribution from the Department of Chemistry, University of Illinois, Chicago, Illinois 60680,
and the Departamento de Quimica Inorganica, Universidad Autonoma, Barcelona, Spain

Superexchange in Chromium(III) Complexes: A Survey of Magnetic Behavior

RICHARD L. CARLIN,* RAMON BURRIEL, JOSEFINA PONS, and JAIME CASABÓ

Received December 29, 1982

The magnetic susceptibilities at low temperatures of a series of 11 polycrystalline bimetallic coordination compounds of Cr(III) are presented. Materials such as [Cr(H$_2$O)(NH$_3$)$_5$][Co(CN)$_6$] are found to behave as simple paramagnets, while [Cr(H$_2$O)(NH$_3$)$_5$](CuCl$_5$) appears to undergo magnetic ordering at 298 mK. A number of other Cr/Cr compounds, such as [Cr(urea)$_6$][Cr(NCS)$_6$]·3H$_2$O, remain paramagnetic to temperatures as low as 40 mK. Exchange interactions are found to be remarkably weak in most of the compounds investigated. The compound [Cr(C$_5$H$_5$NO)$_6$](ClO$_4$)$_3$ also exhibits very weak exchange interactions.

Introduction

There are relatively few known superexchange-coupled antiferromagnets of chromium(III), so we have begun a search for new ones. The major reason for doing so is that chromium is one of the few examples of an $S = {}^3/_2$ ion, which means that zero-field splitting effects can be important for its magnetochemistry. So much of the subject of magnetism has been restricted to copper(II) ($S = {}^1/_2$ and therefore a quantum ion), manganese(II) ($S = {}^5/_2$ and therefore nearly a classical spin ion), and cobalt(II) (effective $S = {}^1/_2$ in all cases studied to date at low temperatures, whether octahedral or tetrahedral in geometry). Nickel(II) is of course intermediate, with $S = 1$, but most of the experimental studies to date on $S = {}^3/_2$ systems have centered around the unusual molecule FeCl(S$_2$CNEt$_2$)$_2$.[1,2] Such systems as CrCl$_3$ ($T_c \sim 16.8$ K), CrBr$_3$ ($T_c \sim 32$ K), and Cr$_2$O$_3$ ($T_c \sim 308$ K) order at temperatures too high for the zero-field splitting of the $^4A_2$ ground state to affect in any way the magnetic character of the systems. The Cr alums order at very low temperatures, principally by dipolar interactions. So, it appeared reasonable to us to search for new (superexchange) antiferromagnets of chromium(III) whose magnetic interactions became important at intermediate temperatures, especially in the temperature range accessible to us (40 mK–20 K). A great deal of theory for $S = {}^3/_2$ has already been done, but little of it includes crystal-field splitting terms. These become evident in some of our measurements even though the zero-field splitting with chromium is almost always smaller than 1 K.

Studies of [Cr(NH$_3$)$_6$](ClO$_4$)$_2$Br·CsBr, for example, showed that magnetic exchange is particularly weak in this material. Susceptibilities measured down to 40 mK allowed us[3] to evaluate the zero-field splitting parameter $2D/k$ as 0.53 K, but magnetic ordering was not found.

Table I. Heterobimetallic Chromium(III) Compounds[a]

	$\langle g \rangle$	$\Theta \pm 0.05$, K
[Co(NH$_3$)$_6$][Cr(CN)$_6$]	1.97	0
[Cr(H$_2$O)(NH$_3$)$_5$][Co(CN)$_6$]	1.93	−0.08
[Co(H$_2$O)(NH$_3$)$_5$][Cr(CN)$_6$]	1.92	0.02
cis-[Cr(H$_2$O)$_2$(NH$_3$)$_4$][Co(CN)$_6$]	1.83	0
[Cr(H$_2$O)(NH$_3$)$_5$](CuCl$_5$)	1.97	−0.15

[a] From data taken over the temperature interval 1.2–4.2 K.

The compound Cs$_2$CrCl$_5$·4H$_2$O is more interesting because it does undergo magnetic ordering at 180 mK.[4] Magnetic exchange and the zero-field splitting appear to be comparable in magnitude; we found $D/k = -0.16$ K, $E/k = -0.05$ K, and $zJ/k = -0.09$ K. The compound exhibits lower dimensional behavior.

An early study[5] observed that exchange interactions were very weak in the common compound [Cr(NH$_3$)$_6$]Cl$_3$, for the magnitude of the Weiss constant was less than 0.01 K. The compound [Cr(NH$_3$)$_5$Cl]Cl$_2$ was found to obey the Curie–Weiss law down to 1.5 K with $\Theta = -0.8$ K; magnetic ordering has not yet been reported for either compound. One may compare these results with those on [Ni(NH$_3$)$_6$]Cl$_2$[6] and [Ni(NH$_3$)$_6$](NO$_3$)$_2$,[7] for example, which have respective ordering temperatures of 1.02 and 1.35 K.

We recently reported[8] that superexchange interaction in some chromium(III) salts can be enhanced by the presence

---

* To whom correspondence should be addressed at the University of Illinois.

(1) De Fotis, G. C.; Palacio, F.; Carlin, R. L. *Phys. Rev. B: Condens. Matter* **1979**, *20*, 2945.

(2) De Fotis, G. C.; Cowen, J. A. *J. Chem. Phys.* **1980**, *73*, 2120.

(3) Chirico, R. D.; Carlin, R. L. *Inorg. Chem.* **1980**, *19*, 3031.

(4) Carlin, R. L.; Burriel, R. *Phys. Rev. B: Condens. Matter* **1983**, *27*, 3012.

(5) Kobayashi, H.; Haseda, T.; Mori, M. *Bull. Chem. Soc. Jpn.* **1965**, *38*, 1455.

(6) van Kempen, H.; Duffy, W. T., Jr.; Miedema, A. R.; Huiskamp, W. J. *Physica (Amsterdam)* **1964**, *30*, 1131.

(7) Beccera, C. C.; Sano, W.; Marques, A.; Frossatti, G.; Paduan Filho, A.; de Oliveira, N. F., Jr.; Quadros, C. J. A. *Phys. Lett. A* **1972**, *40*, 203.

(8) Carlin, R. L.; Burriel, R.; Pons, J.; Casabo Gispert, J. *Inorg. Chem.* **1982**, *21*, 2905.